Report on DESY SSP 2011 activity

SiPM Light Mixers for CMS HO Upgrade

Artur Lobanov *

Moscow State University, Russia

DESY CMS Group

Supervisor: Benjamin Lutz

Abstract

During this programme, I have been working in the HO (HCAL Outer) group of CMS DESY. The research was concerned with the future upgrade of the outer hadronic calorimeter, which requires the substitution of HPDs (Hybrid Photo Diode) with SiPMs. Due to the different aperture sizes of these detectors, a coupling light guide (called light mixer) is required.

Several different LM have been developed. My task was to analyse the data from the July 2011 test beam at SPS and provide measurements in the DESY lab to choose the best performing light mixer.

2011, Hamburg

*e-mail: arturlbv@gmail.com, artur.lobanov@desy.de

Contents

1 Intro

1.1 The CMS Detector

CMS [***C**ompact* ***M**uon* ***S**olenoid*] is a 4π general-purpose detector capable of studying many aspects of proton collisions at 14 TeV, the center-of-mass energy of the LHC particle accelerator.

It contains subsystems which are designed to measure the energy and momentum of photons, electrons, muons, and other products of the collisions. The innermost layer is a silicon-based tracker. A scintillating crystal electromagnetic calorimeter is surrounding it, which is itself surrounded with a sampling calorimeter for hadrons. The tracker and the calorimetry are compact enough to fit inside the CM Solenoid which generates a powerful magnetic field of 3.8 T. Outside the magnet are the large muon detectors, which are inside the return yoke of the magnet.

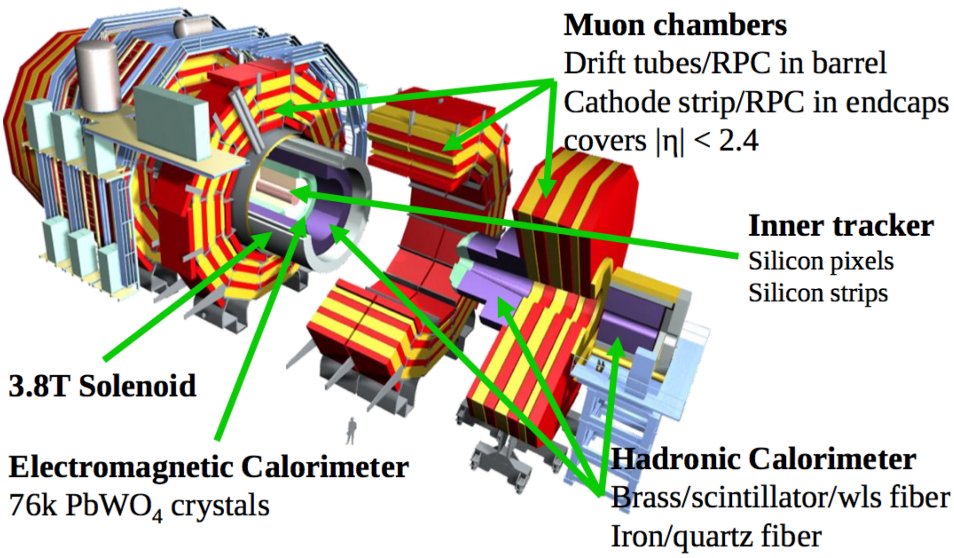

Fig. 1: The CMS detector

1.2 CMS HCAL

The hadron calorimeters in conjuction with the ECAL subdetectors form a complete calorimetry system for the measurement of jets and missing transverse energy [3]. The central barrel and endcap HCAL subdetectors completely surround the ECAL and are fully immersed within the high magnetic field of the solenoid (Fig. CP 1). The barrel (HB) and endcap (HE) are joined hermetically with the barrel extending out to $|\eta| = 1.4$ and the endcap covering the overlapping range $1.3 < |\eta| < 3.0$. The forward calorimeters are located 11.2 m from the interaction point and extend the pseudorapidity coverage overalapping with the endcap from $|\eta| = 2.9$ down to $|\eta| = 5$. The forward calorimeters (HF) are specifically designed to measure energetic forward jets optimized to discriminate the narrow lateral shower profile and to increase the hermeticity of the missing transverse energy measurement. Central shower containment in the region $|\eta| < 1.26$ is improved with an array of scintillators located outside the magnet in the outer barrel hadronic calorimeter (HO).

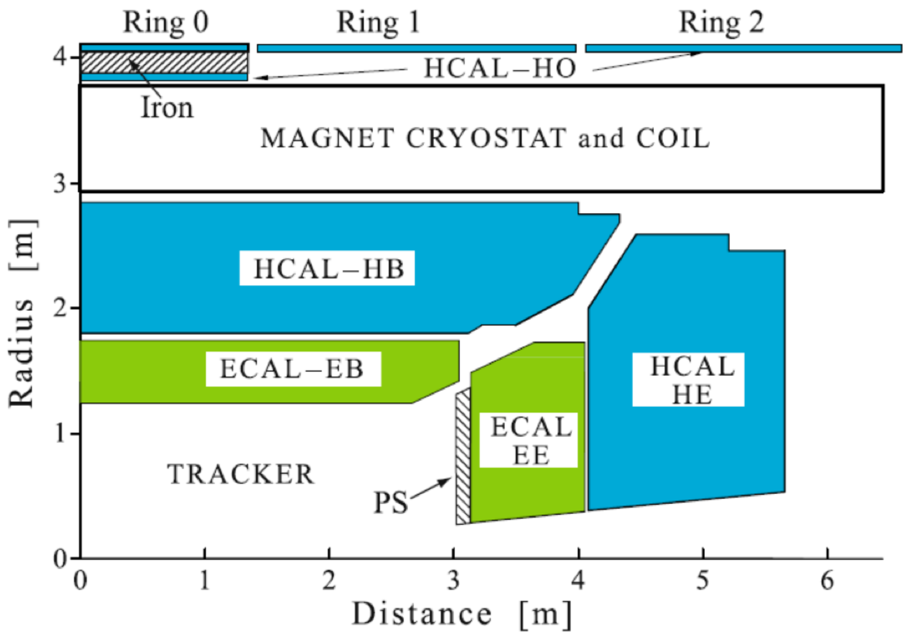

Fig. 2: The CMS Hadronic Calorimeter

1.2.1 HCAL Outer

The HCAL Outer (HO) represents a "tail catcher" for the barrel calorimeter which is required due to the nonsufficient thickness of the barrel of less than $10\lambda_0$. Hadronic showers, especially those starting relatively late in the HCAL, may leak into the magnetic coil and the return yoke and lead to a wrong reconstruction of the shower energy.

An aditional layer of the calorimeter, placed behind the magnetic coil and outside of the cryostat, the HO helps to interpret the shower and corrects missing E_T and jets particularly in Ring 0. Figure 3 shows the HCAL material budget improvement with HO in units of interaction lenghts.

As muons propagate through all subdetectors and leave a specific small signal, HO can be used to identify muons as well.

HO has the same structure as the sample tiles of the barrel part of HCAL. The scintillation signal goes through a fibre into an Optical Decoder Unit (ODU), which is coupled to a Hybrid Photo Diode (HPD).

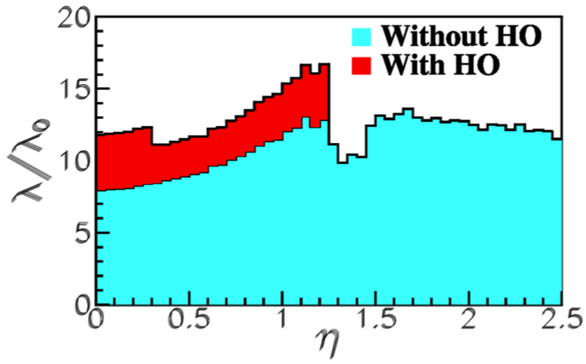

Fig. 3: HCAL material budget

1.3 HO Upgrade

While the HPD works well in high magnetic field of the barrel, it is too sensitive for consistent, reliable operation in the less well determined fields of the return yoke. The HPDs of the HO have had problems since their initial cosmic running with the full magnetic field. Currently the HPDs in Ring 0 are working at lower power voltages that allow safe operation of the HPDs. The Ring 2 HPDs are disabled, because of the stronger magnetic stray field.

Because of these problems CMS has decided to replace the HPD sensors with magnetic field-resistive Silicon Photomultipliers (SiPM). As the SiPMs have also other advantages compared to HPDs, this will bring the HO up to and exceed design sensitivity.

This represents the first large scale application of SiPM sensors to a collider experiment.

1.3.1 Silicon Photo Multipliers

The Silicon Photomultiplier is a multipixel semiconductor photodiode, where the pixels are joint together on common silicon substrate. Each SiPM pixel operates in limited Geiger mode (Avalanche Photo Diode), under bias voltage of few volts above more than breakdown voltage, so each electron-hole pair generated by photons gives rise to a Geiger-type discharge. This Geiger discharge is stopped when the voltage goes down below breakdown value due to a external resistor on each pixel. This resistor also serves as a decoupling element between the individual pixels.

This mode allows pixels to âĂIJcountâĂİ photons: $\text{signal} \propto \sum \text{cells fired}$. But in opposite to an almost linear response of a common PMT, the SiPM saturates as more photons hit more pixels as a hit pixel takes some time to recover to full sensitivity. Additionally, as SiPMs are semiconductor-based, they show high temperature sensitivity and radiation damage.

But allover in comparison to PMTs/HPDs, the SiPM advantages are:

- insensitivity to magnetic fields

- better signal to noise
- eliminate 8kV HV supplies and maintenance

1.3.2 Light Mixers

Basically, the need in light mixers is because of the different aperture of the ODU output fibres and SiPM size. An ODU "pixel" has the size of 3.8mm, whereas a SiPM sensor is 3mm $\times$ 3mm (3600 pixels). Of big importance is also the ability of LMs to mix light coming out of different fibres and distribute it over the whole SiPM surface to decrease saturation.

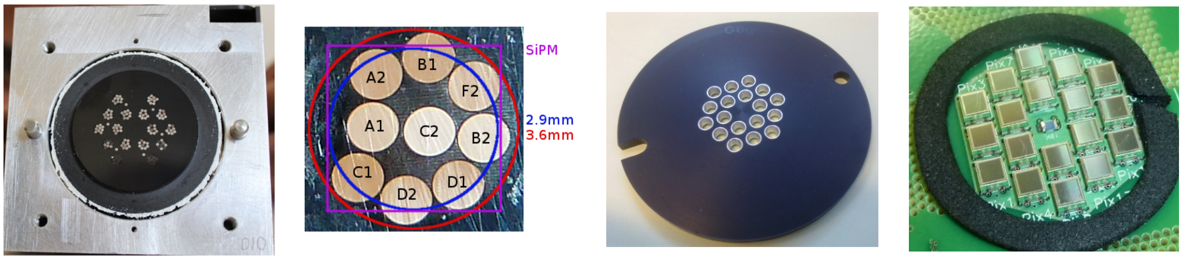

a) b) c) d)

Fig. 4: a) – ODU, b) – LM, c) – SiPMs

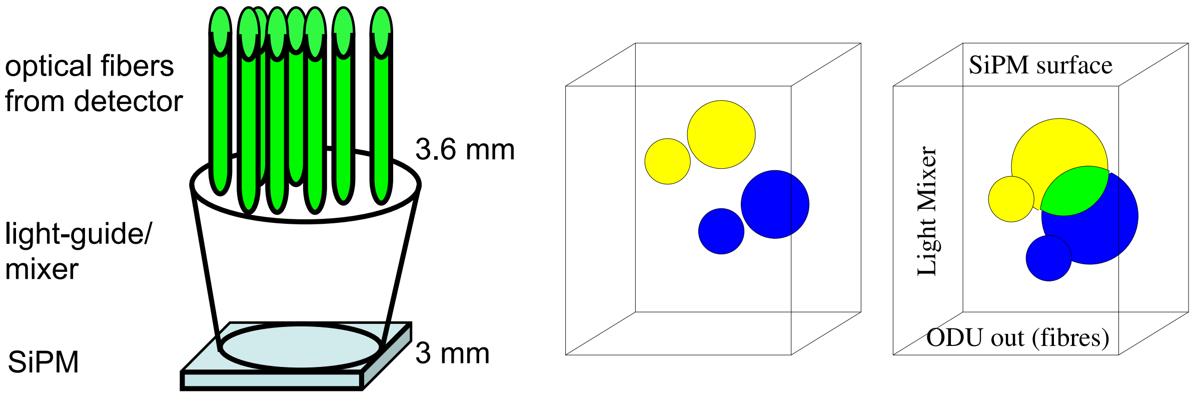

a) b) c)

Fig. 5: a) – LM working scheme, b) – no mixing, c) – mixed signals

In order to estimate the mixing capabilities of a LM, let us consider two cases:

1. For far away fibres/thin LM the light cones do not intersect on the SiPM surface. The individual signals are e.g. A_1 and A_2.
   Then the total signal is $A_{tot} = A_1 + A_2$.

   Saturation is $\propto$ the number of fibres: $= N_{fibres} \times A_{max,fib}$

2. For near fibres/thick LM the light cones intersect on the SiPM surface, which leads to a smaller lit area.
   Then the total signal is not the sum $A_{tot} \neq A_1 + A_2$.
   In the limit of ideal mixing $= A_{max,SiPM}$ (SiPM's own saturation)

This comparison shows, that thicker LMs will mix light the best way, but also light loss, which also grows with the thickness of the LM, should be taken into account.

2 Test Beam Analysis

2.1 Test Beam Setup

The test beam was held at the H2 beam line of SPS in CERN. Mostly, pions and muons of different energies were used. A CMS slice prototype was used as a detector. It contained the Electromagnetic and Hadronic Calorimeters (Barrel, Forward and Outer). As HO's Ring 2 optics are identical to Ring 1, only R1 and R0 were tested. The bench was able to rotate, so that the particle could be directed to various tiles.

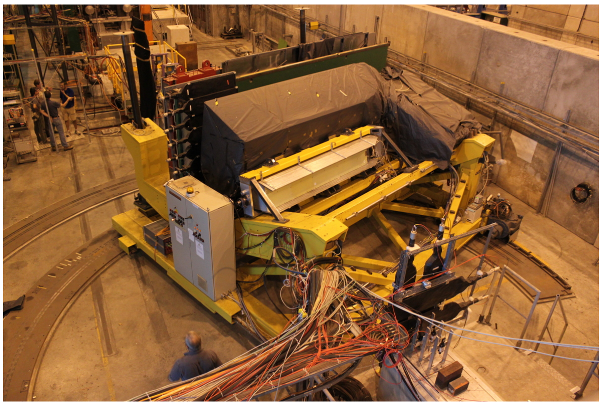

Fig. 6: Test Beam setup showing CMS HCAL slice

As the data amount taken during the Test Beam is huge, the whole analysis was ran at the National Analysis Facility (NAF) at DESY. The framework of CMS, CMSSW, was used to process the raw data. ROOT was also used for analysis of all data.

2.2 Analysis Algorithm

For the following analysis only 150 GeV muon runs were used.

The signal from the readout modules (RM) comes in 25ns timeslices, which is specified by the CMS framework [I left this], as the basic timing of the LHC clock is 40 MHz.

Due to the different timing in HPD and SiPM response, the signal integral is calculated over different timeslices.

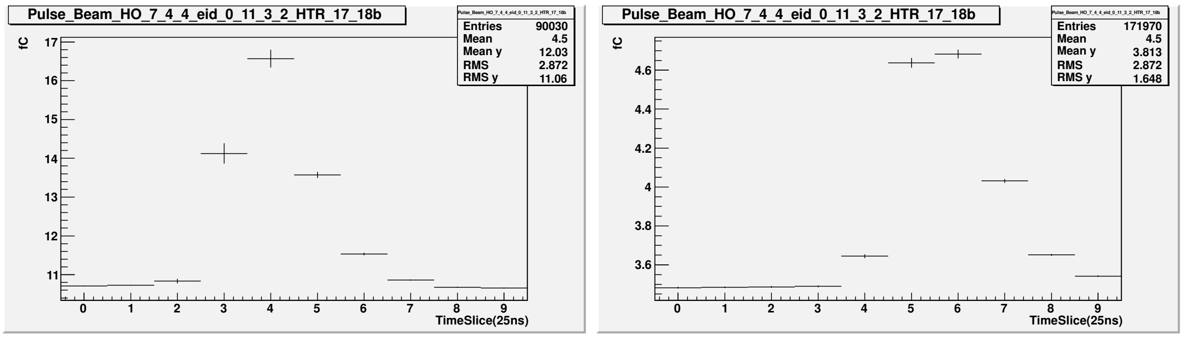

Fig. 7: HPD vs. SiPM timeslices

The event record contains the energy deposit (integral of signal) of every module position in HO, HB, HF, and also the trigger ID which was fired for the corresponding event. A typical raw signal distribution for one HO segment is shown in fig. 8.

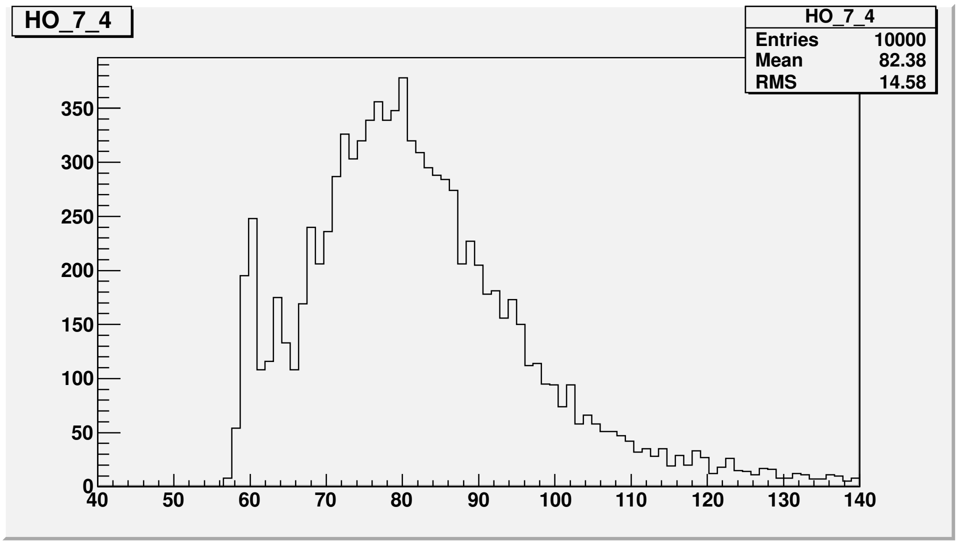

Fig. 8: HOenergy for one position ($\eta = 7, \phi = 4$) without triggers

Using the trigger information the raw signal can be devided into pedestal and true signal events, which is shown in fig. 9.

The HO signal by itself has the form of a Landau distribution, but due to electronic noise and the use of a thick scintillator it gets a convoluted function of a Landau and Gaus distribution, like:

$$\int_0^t \varphi(s)\psi(t-s)\,ds$$

So the convuluted function looks like

$$\int_0^t Landau(s) \times Gaus(t-s)\,ds$$

Due to the single-electron peaks on the right side of the pedestal, which are practically noise, the pedestal is being fitted only on its left side.

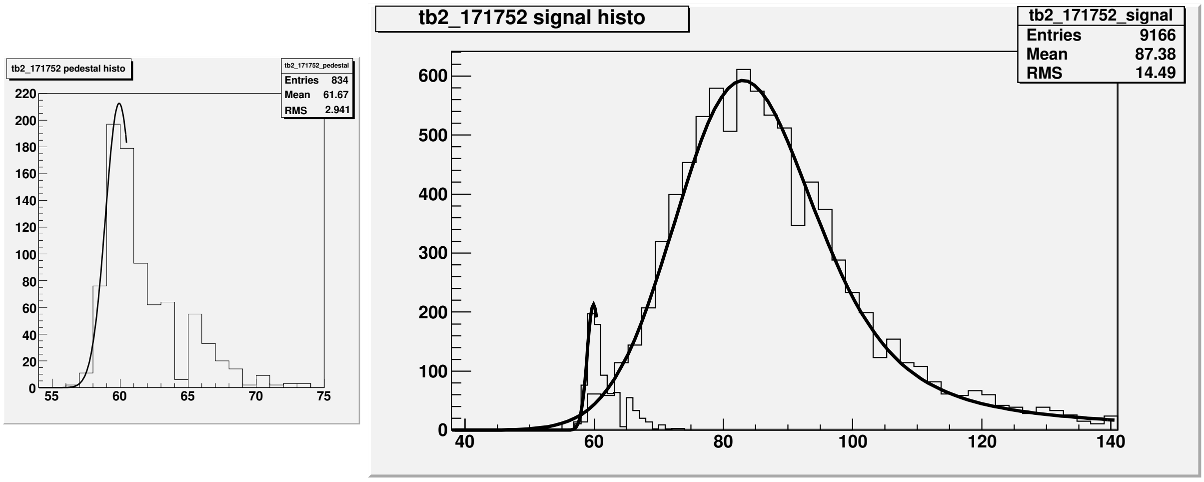

Fig. 9: Gaus fit of pedestal and convoluted landau and gaus fit of signal

The Most Probable Value of the convoluted function gives the mean signal value for each run. Signal to noise ratio is determined from the MPV and width of pedestal.

2.3 Light Mixer Comparison for Ring 1 & 0

For the LM performance comparison the signal and pedestal width for each run was calculated. To have an averaged value for one tower the mean signal for the runs inside of the tower was taken.

Tables 1 & 2 show, that the least light loss relative to bare SiPM is for the 3mm NotreDame LM (20%), which is followed by DESY 2mm (23%). The biggest light loss is approx 40 % for DESY 3mm. NotreDame 4m loses about 30%.

Though the signal to noise ratio is overestimated, one can say that, for real application, it will still be higher than the required value of 5. This is significantly higher, than the HPD S/N.

A look at the absolute signal values raises an issue - the signal in tower 7-3 is twice as large as in 7-4. Comparing other towers could show some trend.

2.3.1 Signal variance over towers

Fig. 10 shows the absolute signal distribution for different towers of Ring 1. An inhomogeneous picture, showing large random deviations can be seen. As in this case the SiPM is coupled directly to the ODU, this can't be a LM problem, but rather could be related to voltage or temperature instabilities. In fig. 10 one can see the relative LM to bare signal for vaious Ring 1 towers. The best homogeneity is observed for the DESY 2mm LM. The only significant deviation is seen in tower 7-4 which shows big deviations for all other towers, too. This could point to some systematic error during

Table 1: Mean values for tower $\eta = 7, \phi = 4$ (Ring 1)

PM	LM	Signal [fC]	% of bare	σ_{pedestal}	Sig/noise [1]
SiPM	bare	26.87	100	1.09	25.06
SiPM	DESY 2mm	20.57	77	1.06	19.40
SiPM	DESY 3mm	17.03	63	0.96	17.57
SiPM	NotreDame 3mm	22.17	82	1.01	21.95
SiPM	NotreDame 4mm	18.89	70	1.01	18.90
HPD	–	2.59	–	1.15	2.25

Table 2: Mean values for tower $\eta = 7, \phi = 3$ (Ring 1)

PM	LM	Signal [fC]	% of bare	σ_{pedestal}	Sig/noise [1]
SiPM	bare	56.28	100	1.29	43.64
SiPM	DESY 2mm	42.31	75	1.21	38.36
SiPM	DESY 3mm	34.46	61	1.21	28.64
SiPM	NotreDame 3mm	44.16	78	1.27	35.03
SiPM	NotreDame 4mm	33.57	60	1.28	26.19

Table 3: Mean values for position $\eta = 2, \phi = 3$ (Ring 0)

PM	LM	Signal [fC]	σ_{pedestal}	Sig/noise	% of bare[2]
SiPM	DESY 7mm	28.00	1.06	26.40	33
HPD	–	0.63	1.20	0.52	

Table 4: Mean values for position $\eta = 2, \phi = 5$ (Ring 0)

PM	LM	Signal [fC]	σ_{pedestal}	Sig/noise	% of bare[2]
SiPM	DESY 3mm	45.40	0.94	48.24	53
HPD	–	2.87	1.20	2.40	

the test beam data was taken. Overall, the other LM look less uniform, than DESY 2mm.

As no bare SiPM runs were available for Ring 0, we had to use the doubled mean value of the bare signal from Ring 1, since R0 is double layered. The light loss to bare is significant, whereby the relative 7mm to 3mm loss is about 40 %. This estimation

[1] not accounting electronic noise overestimates this value, which also decreases with radiation damage

[2] bare from Ring1 data: $\frac{A_{\text{LM, R0}}}{2 \times A_{\text{bare, R1}}}$

would be incorrect, if Ring 0 shows similar tower dependent variations for the signal as Ring 1. Still, the signal to noise ratio is rather good and exceeds the value for HPDs. For tower 2-3 the HPD signal is absent. This issue is also observed by other collaborators.

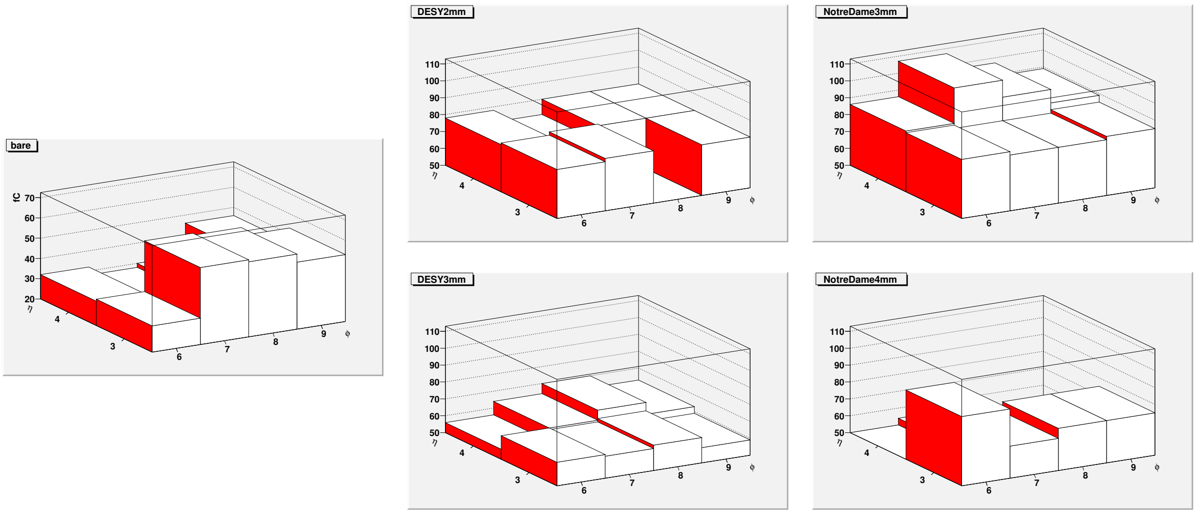

Fig. 10: Mean SiPM signals for Ring 1 towers

2.3.2 Spatial distribution of signals for one tower

A more detailed look at the signal distribution inside of a Ring 1 tower can be seen in 2.3.2 tables. The general issue comes from all distributions – no common trend is observable. Possible reasons could also be HV, temp instabilities or optical coupling variance. An estimation of difference of fibre lightguiding quality was done at the DESY laboratory (see 3.2).

Fig. 11: DESY 2mm

+0.5		+4.0
	+4.5	+3.0
-6.0		-0.3

Fig. 12: DESY 3mm

-4.6		+1.3
	+4.0	+0.1
-4.0	+3.1	-4.3

Fig. 13: NotreDame 3mm

-2.7		+1.3
		+4.0
-0.8	-0.8	-0.4

Fig. 14: NotreDame 4mm

+1.5		+9.1
		+11.9
-0.6	-21.5	-(.1;9.4)

Fig. 15: bare SiPM

-4.2		+1.2
	+2.2	+6.6
-1.9	+2.0	-6.2

Fig. 16: HPD

	+4.9	+3.0
-7.0	0	-2

Fig. 17: Signal deviation inside of one tower for each LM, bare SiPM and HPD

3 Laboratory Measurements

3.1 Laboratory Setup

The test setup is constructed at the CMS laboratory at DESY. Its principle is, that light from LEDs is transmitted to an ODU like in HO at CMS itself, where the light is being detected by the SiPMs. The source and detector are placed in two different black boxes and connected through an optical cable.

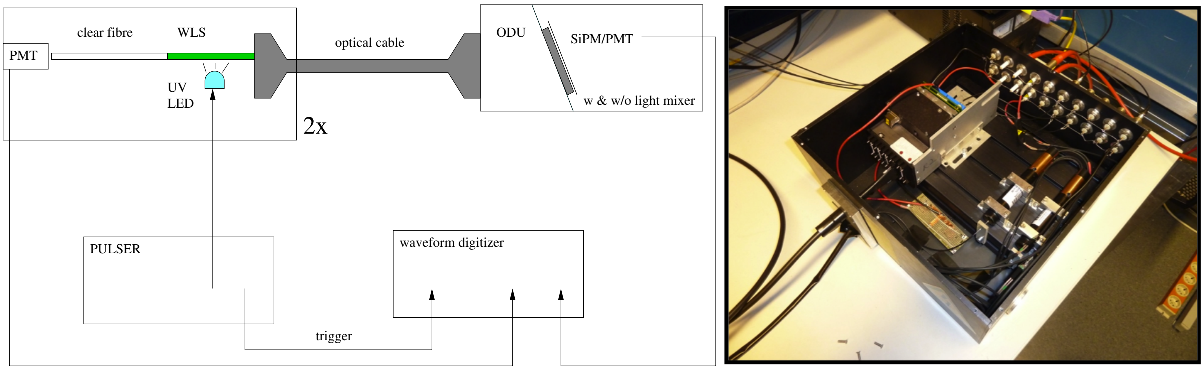

Fig. 18: Laboratory test setup

- The LED black box has 2 UV LEDs, which are shining on a wavelength-shifting fibre through an aperture changing adaptor. These adaptors allow us to change the LED light intensity.

  Both ends of the WLS fibres are coupled to clear fibres and extracted from the black box.

- The Sensor black box has an ODU and 2 PMTs. One end of each fibre is coupled to the ODU, the other goes to a reference PMT, so that the light coming to the SiPM could be monitored through the linear (under this conditions) PMT.

  The box has also plugs for an additional PMT, which can be coupled to the ODU instead of the SiPM.

A SRS DG645 serves as a pulse generator for the LEDs (named AB & EF after the generator's output channels) and trigger for the readout ADC from CAEN. The signal can be checked visually by a Tektronix TDS3054 oscilloscope. The SiPM high voltage power supply is provided by Rhode & Schwarz. A 40 channel HV CAEN supplies the PMT HV. For SiPM signal amplification two THS4303EVM units are used.

Though the ODU has 10 plugs á 16 fibres, only 9 are used as they point to one SiPM, which equals to 1 readout-channel. The 9 fibres are distributed over 5 plugs: 4 with two active fibres and 1 with a single one. Both fibres in a plug can be lit simultaneously.

3.2 Light Yield Comparison for Fibres and LMs.

As the Test Beam data analysis has shown, a big variance in amplitude is observed within one tower, which corresponds to a single ODU pixel (fibre bundle), it was decided to investigate the light yield dependence for different fibres within one ODU pixel.

For this measurement a PMT is coupled to the ODU – this guarantees, that the photo-sensor has a large aperture compared to the fibre bundle. High LED amplitudes are required to get a stable and reliable PMT response. The mean signal for the amplitude distribution represents the light intensity, registered by the PMT.

The resulting graph is shown in fig. 19. One can see, that different fibres show significant variations in transmission. The largest deviation is up to 15%. But as the deviation behaves like $\frac{1}{\sqrt{N}}$ for a N fibre bundle, 4 fibres would already decrease it by a factor of 2. Such a results gives reason to assume, that the big signal variance in the Test Beam data could not come only from different fibre couplings.

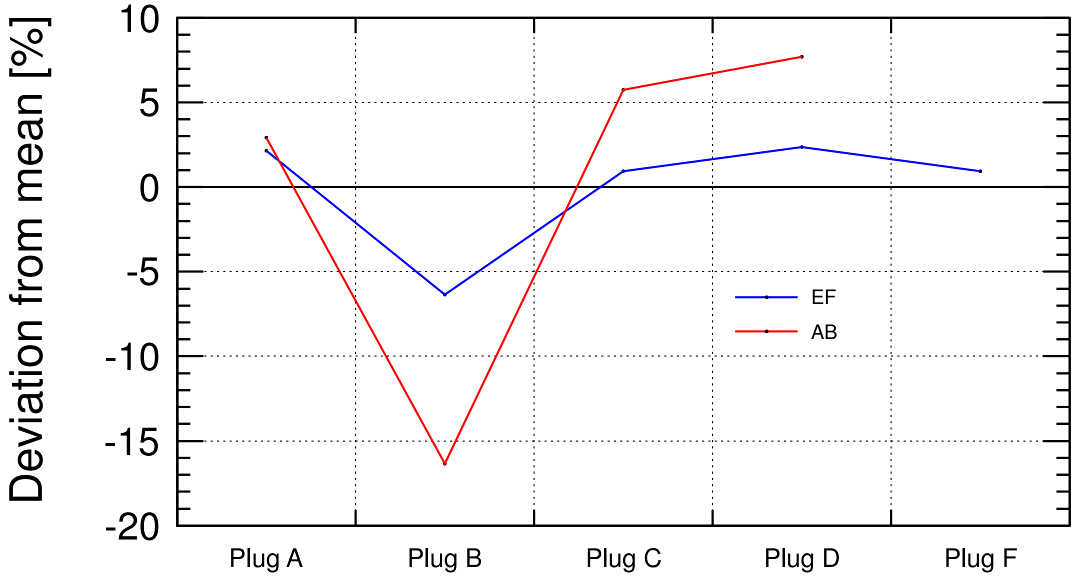

Fig. 19: Light loss in different fibres [measured with PMT]

Besides the light loss in coupling, the light loss for different light mixers was measured. As the light yield defines the signal to noise ratio, it is essential to know about the light loss characteristics for the LM. The SiPM signal got amplified 50 times to improve the readout sensibility of the ADC.

This measurement is done by exchanging LMs and recording the SiPM signal at low LED amplitudes to prevent any saturation of the sensor. The mean signal for the amplitude distribution represents the light intensity, registered by the SiPM.

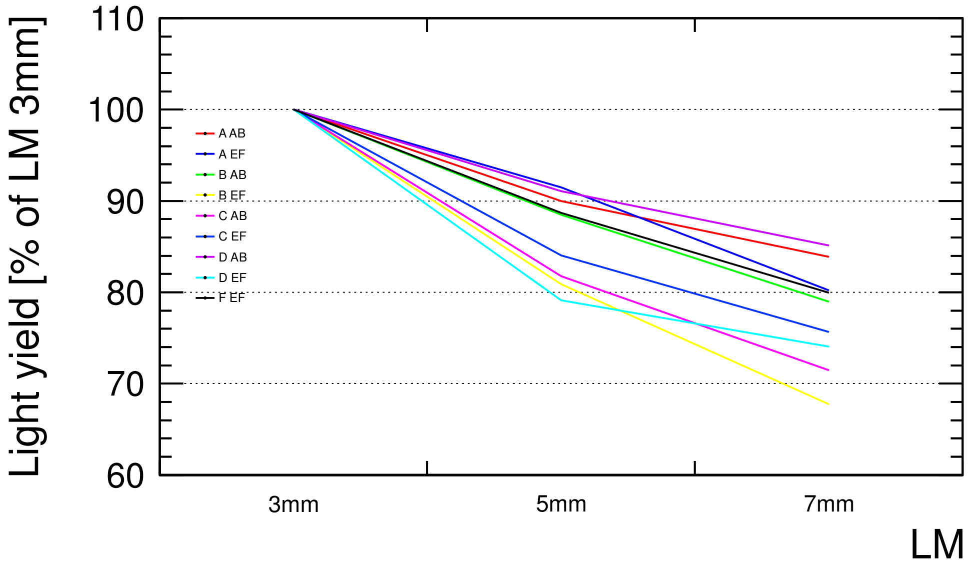

Fig. 20: Light loss comparison for LMs [for SiPM]

As seen in fig. 20, the light yield drops with the LM thickness. This is expected due to the increasing light-way length, causing a bigger probability of absorbtion. An average loss for LM5mm $\approx 15\%$, LM7mm $\approx 22\%$ relatively to LM3mm is measured. Taking into account the measurement accuracy, this could agree with the TB data, which for 7mm to 3mm is 38%.

3.3 Saturation Measurements

Another important characteristic of the LMs is their ability to actually mix the light and improve the saturation performance of the SiPM (as shown in fig. 5). This measurements differ from the previous ones because the same light pulse is also measured by PMTs. In the used signal range the photomultipliers are assumed to be linear and don't saturate so that they can be used as a reference for the SiPM signal. The measurement is done not only for the single LEDs but also for their combination, which allows to evaluate the mixing capabilities of the LMs. A resulting graph is shown in fig. 22.

In addition, a gain measurement was done. For this a low LED signal was sent to the SiPM so that only a few pixels are fired. The gain is then calculated from the distance between the single-electron peaks (as shown in fig. 21).

In order to get a clear view of the difference in saturation for the various LMs, we have to renormalise the axes of the saturation curve. For saturation measurements we can disregard the (absolute) transmission efficiency, so we calibrate the curves in 2 steps:

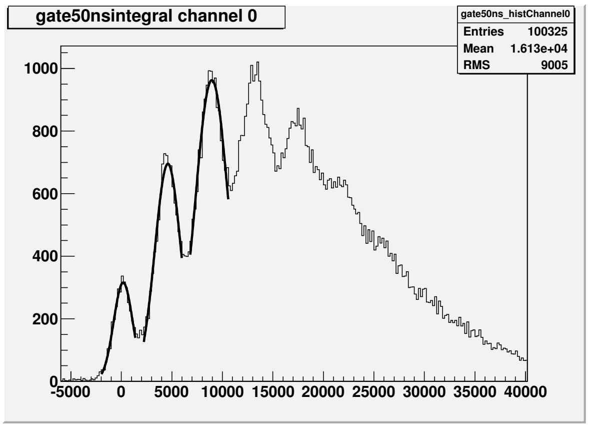

Fig. 21: SiPM signal distribution at low intensity for gain calculation

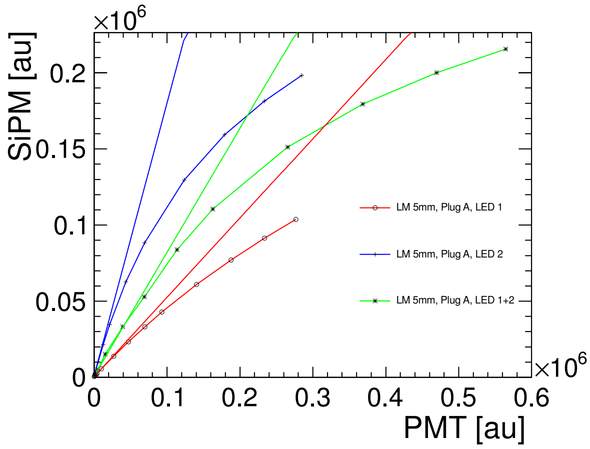

Fig. 22: Non-calibrated curves

1. Y-axis: the signal is divided by the gain [in ADC counts] to show the actual number of pixels fired (and thus the scale of saturation)
2. X-axis: the input signal is transformed to “linearised pixels", which means, that all curves have the same behaviour in the low-signal region, where linearity is assumed. This also allows us to directly add the signals of the two PMTs.

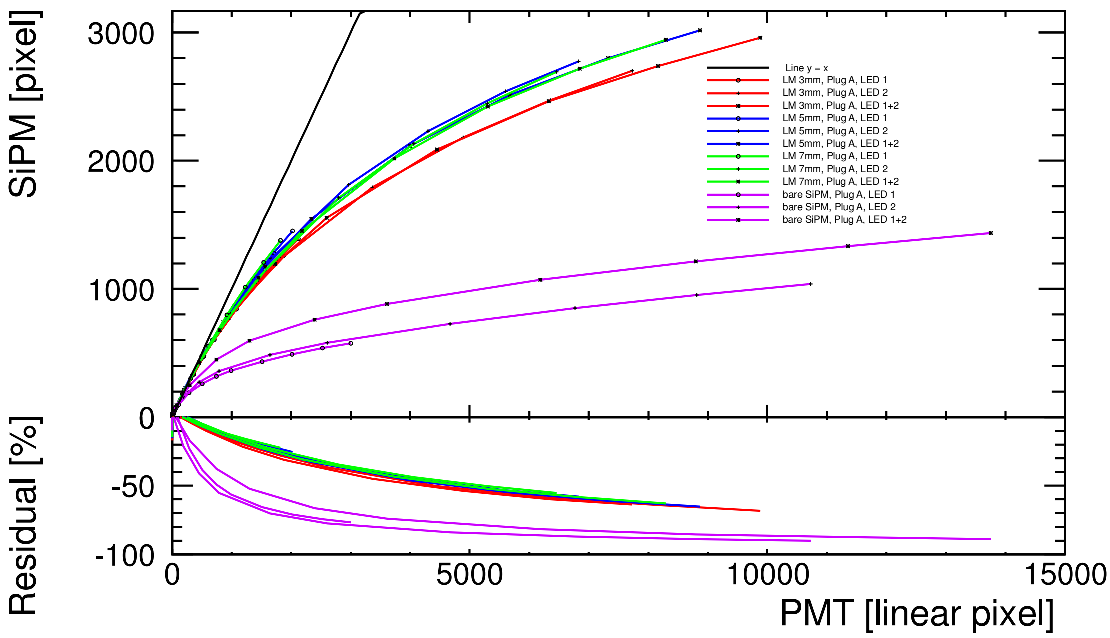

Fig. 23: Saturation curves for all light mixers at plug A

Figure 23 shows the saturation curves for all LMs after calibration. A clear benefit from the LM can be seen: the light covers a bigger surface so more pixels are fired. For instance, for an accepted 50% nonlinearity the LMs show 8-times higher dynamic range.

Also here one can see, that the saturation curve for LM3mm goes to higher X-values, than LM5mm, which points to the fact, that the thinner the light mixer is, the more light reaches the SiPM.

Mixing comparison

The mixing performance for different LMs can be seen, when comparing the saturation curves for different fibre constellations: when they are near by each other, and when they illuminate different parts of the SiPM.

As fig. 24 corresponds to plug A, the fibres A1 and A2 (see fig. 5, b) are close to each other. In this case we do not see any difference in mixing for the various LMs.

But for plug C, which has the fibres C1 and C2, one can see, that the single LED curves for LM 3mm add up, which corresponds to worse mixing, than LM5mm and LM7mm, which is due to the small thickness.

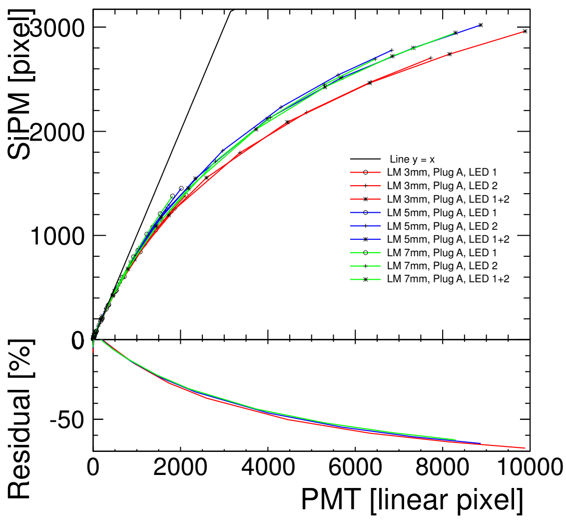

Fig. 24: Saturation curves for plug A [fibres near]

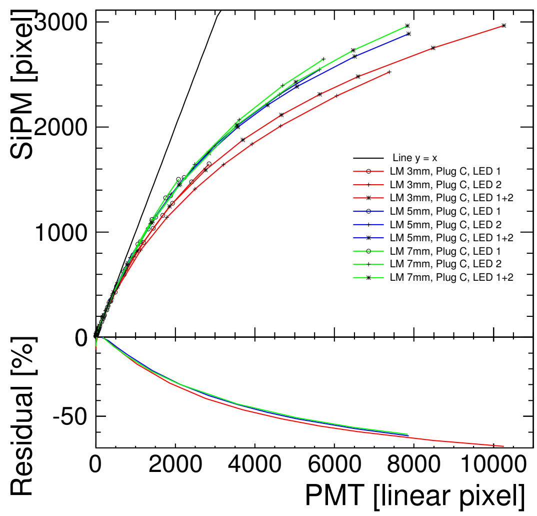

Fig. 25: Saturation curves for plug C [fibres far]

4 Summary

The HCAL Outer represents a “tail catcher" for HB, which is supposed to contain hadronic showers. As HPDs, which collect the scintillation light from the HO tiles, are sensitive to the not well known magnetic field in the return yoke, their operation is almost impossible. It was decided to replace HPDs with SiPMs, which are magnetic field insensitive. To use the existing readout mechanics and improve the light distribution over the SiPM surface, special light mixers were created. Two different approaches to LM testing were implemented – test beam analysis & test bench measurements. The results are the following:

- Light transmission:
  - Large fibre-to-fibre and channel-to-channel signal variations have been measured.
  - The LM caused light loss is significant – it varies from 20% to 40%.
- Saturation:
  - The single coupled fibres saturate at 400 pix, what gives an expected saturation limit for Ring 1 & 2 at $\approx$ 1600pix.
  - In Ring0: LM3mm performs not optimal, but better, than bare SiPM. Starting from 5mm and higher give an optimal mixing for R0.
  - The expected saturation limit for fired pixel equals the LM inner radius fraction on the SiPM surface $= \pi \frac{(\frac{2.9mm}{2})^2}{3mm \times 3mm} \times 3600 \approx 2600$, coming close to data.
- Saturation correction:
  - The bare coupling behaves like EDU (electronic DU) in HB.
  - With a light mixer it behaves more like ODU in HB.
  - A saturation correction is possible for good mixing LMs, whereas bad mixing might require single channel calibration.

Acknowledgements

First of all, I would like to thank my supervisor Benjamin Lutz for this interesting project and all the support he provided. This time was really cognitive and useful for me. Benjamin taught me the principles of this topic, showed me how to work with the CMS software and do data analysis using the NAF, how to make laboratory measurements. He also helped me to improve my programming skills.

Also I would like to thank Isabell Melzer-Pellmann for introducing me to DESY and SUSY. Our joint battle against evil ROOT with Elias Ron during my first physics analysis attempts are not to be forgotten, too.

Special thanks go to our organizers – Olaf Behnke, Doris Eckstein and Andrea Schrader. Thank you very much for making this programme as good as it was for us. This experience was wonderful and inspiring. I wish you good luck with this programme in the future!

Last, but not least, I would like to thank my office/kitchen-mate Sophie and ROOT-co-victims Alina, Sarah and Alex for their company during the office hours, and also all all other Summer Students (here should be the list of all summies-names) for making this summer time completely awesome and unforgettable.

References

[1] Jake Anderson, *Upgrade of the CMS Hadron Outer Calorimeter with SiPM's*. Fermilab, TIPP 2011.

[2] P. Buzhan, B. Dolgoshein, et al., *An Advanced Study of Silicon Photomultipliers*. ICFA Instrumentation Bulletin, 2001.

[3] Y. Musienko, *Advances in multi-pixel Geiger mode APDs (Silicon Photomultipliers)*. INSTR-08, Novosibirsk, 2008.

[4] CMS Collaboration, *CMS Physics TDR*. Volume I: CERN-LHCC-2006-001, 2 February 2006.